EMC/EMI Problems and Diffraction Modeling: Finite Difference Time Domain vs. Method of Moments

Mehmet Alper Uslu
Dept. of Electronics and Communications Engineering
Dogus University
Istanbul, Turkey
alpuslu@gmail.com

Gökhan Apaydin
Dept. of Electrical-Electronics Engineering
Zirve University, Kizilhisar Campus,
Gaziantep, Turkey
gokhan.apaydin@zirve.edu.tr

Levent Sevgi
Dept. of Electronics and Communications Engineering
Dogus University
Istanbul, Turkey
lsevgi@dogus.edu.tr

***Abstract*—Edge and/or tip diffraction has long been investigated. Early attempts were analytical and called High Frequency Asymptotics (HFA). With the use of computers, numerical approaches have also appeared. In this study, two powerful numerical models, Method of Moments (MoM) and Finite Difference Time Domain (FDTD), are used in diffraction modeling on the canonical wedge scattering problem.**

Keywords—diffraction; high frequency asymtotics; finite difference time domain (FDTD); method of moments (MoM); wedge.

I. INTRODUCTION

The word *scattering* is used to represent all components produced from the interaction of Electromagnetic (EM) waves with objects and includes incidence, reflection, refraction, and diffraction. Mathematical methods, such as Geometric Optics (GO), Physical Optics (PO), Geometric Theory of Diffraction (GTD), Uniform Theory of Diffraction (UTD), and Physical Theory of Diffraction (PTD) can be used if the frequency is high (i.e., when the wavelength is small compared with the interacted object size) [1-3].

GO is a ray-based approach which models incident, reflected, and refracted fields between source and observer. PO is an induced-surface-current based approach and models wave scattering caused by the induced-currents on the illuminated side of the object. Both GO and PO models are incapable of modeling edge and/or tip diffracted fields. These deficiencies were removed with the introduction of diffraction models GTD, UTD, and PTD.

GTD takes into account diffraction everywhere except near critical angles and caustics. UTD can handle diffraction near critical angles but still suffers from caustics. Original PTD is general and can handle diffraction everywhere except near grazing incidence (see [4-8] and Aug. issue of the IEEE AP Magazine for the latest revisit). A very useful MatLab diffraction package has been introduced for the illustration and visualization of all these High Frequency Asymptotics (HFA) approaches [9].

Finite Difference Time Domain (FDTD) approach [10] is an effective method in diffraction modeling. This numerical method was used in modeling the wedge scattering problem [11,12]. A useful MatLab-based FDTD package was also introduced for the visualization of diffracted fields and for comparisons with several HFA models [13].

In this paper, a two-step Method of Moments (MoM) [14-17] approach is introduced for the extraction and visualization of diffracted fields on the canonical wedge scattering problem and results are compared with FDTD method.

II. WEDGE DIFFRACTION MODELING

The non-penetrable wedge diffraction problem is canonical and plays a fundamental role in understanding and construction of HFA techniques as well as for the numerical tests.

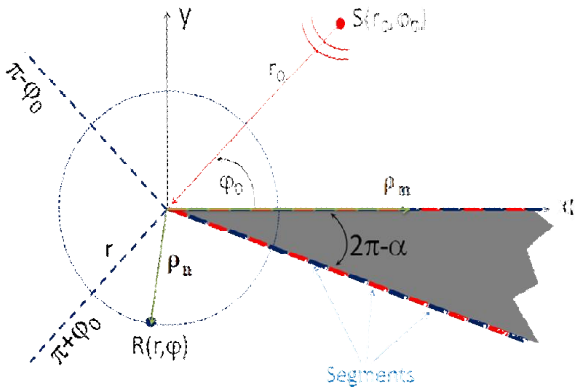

Fig. 1. 2D PEC wedge and segments for scattered fields.

TABLE I. THE EXISTENCE OF FIELD COMPONENTS

Source Illumination	Position of $R(r,\varphi)$	Field Components		
		Incident	*Reflected*	*Diffracted*
SSI ($0<\varphi_0<\alpha-\pi$)	$0\le\varphi<\pi-\varphi_0$	+	+	+
	$\pi-\varphi_0\le\varphi<\pi+\varphi_0$	+		+
	$\pi+\varphi_0\le\varphi<\alpha$			+
DSI ($\alpha-\pi<\varphi_0<\pi$)	$0\le\varphi<\pi-\varphi_0$	+	+	+
	$\pi-\varphi_0\le\varphi<2\alpha-\pi-\varphi_0$	+		+
	$2\alpha-\pi-\varphi_0\le\varphi<\alpha$	+	+	+

The 2D PEC wedge scattering problem in polar coordinates is shown in Fig. 1, where $S(r_0,\varphi_0)$ is the position of the line source, $R(r,\varphi)$ is the position of the receiver point, and α is the exterior angle of the wedge. The *z*-axis is aligned along the edge of the wedge. The angle φ is measured from the top face of the wedge.

According to the position of the line source, either Single-Sided Illumination (SSI) for the illumination of top face ($0<\varphi_0<\alpha-\pi$) or Double-Sided Illumination (DSI) for the illumination of both faces ($\alpha-\pi<\varphi_0<\pi$) can be considered. Table 1 shows the existence of the incident, reflected, and diffracted fields for SSI and DSI cases.

The field outside the wedge satisfies the wave equation, the Boundary Conditions (BC), and the Sommerfeld's Radiation Condition (SRC) at infinity [1]. In the case of acoustic waves, either the field or its normal derivative is zero on the surface and these conditions refer to acoustically soft (SBC) and hard (HBC) wedges, respectively. In the case of EM waves, SBC and HBC correspond to the *z*-component of electric field intensity E_z (TM) and the *z*-component of magnetic field intensity H_z (TE), respectively [12].

The total field solutions of the wave equation with SBC and HBC for both SSI and DSI are [2]:

$$u_s^t=\frac{\pi I_0}{i\alpha}\begin{cases}\sum_{l=1}^{\infty}J_{\upsilon_l}(kr)H_{\upsilon_l}^{(1)}(kr_0)\sin(\upsilon_l\varphi_0)\sin(\upsilon_l\varphi), & r\le r_0\\ \sum_{l=1}^{\infty}J_{\upsilon_l}(kr_0)H_{\upsilon_l}^{(1)}(kr)\sin(\upsilon_l\varphi_0)\sin(\upsilon_l\varphi), & r\ge r_0\end{cases} \tag{1a}$$

$$u_h^t=\frac{\pi I_0}{i\alpha}\begin{cases}\sum_{l=0}^{\infty}\varepsilon_l J_{\upsilon_l}(kr)H_{\upsilon_l}^{(1)}(kr_0)\cos(\upsilon_l\varphi_0)\cos(\upsilon_l\varphi), & r\le r_0\\ \sum_{l=0}^{\infty}\varepsilon_l J_{\upsilon_l}(kr_0)H_{\upsilon_l}^{(1)}(kr)\cos(\upsilon_l\varphi_0)\cos(\upsilon_l\varphi), & r\ge r_0\end{cases} \tag{1b}$$

where I_0 is the line current amplitude, $\upsilon_l=l\pi/\alpha$, and $\varepsilon_0=1/2$, $\varepsilon_1=\varepsilon_2=\varepsilon_3=\ldots=1$. The diffracted fields $u_{s,h}^d$ can be calculated by subtracting the GO fields from (1) in different regions as:

$$u_{s,h}^d=u_{s,h}^t-\frac{I_0}{4i}u_{s,h}^{GO} \tag{2}$$

where

$$u_{s,h}^{GO}=\begin{cases}H_0^{(1)}(kR_1)\pm H_0^{(1)}(kR_2), & 0\le\varphi<\pi-\varphi_0\\ H_0^{(1)}(kR_1) & \pi-\varphi_0\le\varphi<\pi+\varphi_0\\ 0 & \pi+\varphi_0\le\varphi<\alpha\end{cases} \tag{3a}$$

$$u_{s,h}^{GO}=\begin{cases}H_0^{(1)}(kR_1)\pm H_0^{(1)}(kR_2), & 0\le\varphi<\pi-\varphi_0\\ H_0^{(1)}(kR_1) & \pi-\varphi_0\le\varphi<2\alpha-\pi-\varphi_0\\ H_0^{(1)}(kR_1)\pm H_0^{(1)}(kR_3), & 2\alpha-\pi-\varphi_0\le\varphi<\alpha\end{cases} \tag{3b}$$

for SSI and DSI cases, respectively. The distances are:

$$R_1=\sqrt{r^2+r_0^2-2rr_0\cos(\varphi-\varphi_0)} \tag{4a}$$

$$R_2=\sqrt{r^2+r_0^2-2rr_0\cos(\varphi+\varphi_0)} \tag{4b}$$

$$R_3=\sqrt{r^2+r_0^2-2rr_0\cos(2\alpha-\varphi-\varphi_0)} \tag{4c}$$

This model is based on the series summation in (1) and represents reference solution if computed accurately where the critical issue is the specification of the number of terms included which increases with frequency and/or distance.

III. METHOD OF MOMENTS MODELING

Method of Moments (MoM) is one of the earliest frequency domain numerical techniques used in EM [14-15]. Wedge scattering may also be modeled with MoM. In this model, the faces of the wedge are divided into small segments compared to the wavelength (*N* segments top face and *N* segments bottom face). The currents on each segment are assumed to be constant. The source-excited segment fields are calculated and the matrix system is numerically solved and the segment currents are derived. Then, a *2Nx2N* system of equations $[V]=[Z][I]$ is constructed and solved numerically. Here, $[I]$ contains the unknown segment currents, $[V]$ contains segment voltages excited by the source, and $[Z]$ is the *2Nx2N* impedance matrix of the wedge boundary. Then, segment-scattered fields at the observer are accumulated [14].

The MoM-computed scattered fields include reflected and diffracted fields. The diffracted fields can be extracted once reflected fields are available. The reflected-only fields can be obtained from an infinite-plane scenario (i.e., by taking $\alpha=\pi$ and repeating the MoM procedure).

Necessary MoM equations in this procedure are [15-17]

$$V_m=-E_z^{inc}(\boldsymbol{\rho}_n)=-\frac{E_0H_0^{(1)}(kd_n)}{4i}\quad\text{(SBC)} \tag{5a}$$

$$V_m = -H_z^{inc}(\boldsymbol{\rho}_\mathbf{n}) = -\frac{E_0}{\eta_0}\frac{H_0^{(1)}(kd_n)}{4i} \quad \text{(HBC)} \qquad (5b)$$

using distance (d_n) between line source and each segment

$$d_n = \sqrt{[x(\boldsymbol{\rho}_\mathbf{n}) - r_0\cos\varphi_0]^2 + [y(\boldsymbol{\rho}_\mathbf{n}) - r_0\sin\varphi_0)]^2} \qquad (6)$$

and the impedance matrix is obtained

$$Z_{nm} \cong \begin{cases} -\frac{k\eta_0\Delta\rho}{4} H_0^{(1)}\left(k|\boldsymbol{\rho}_\mathbf{n} - \boldsymbol{\rho}_\mathbf{m}|\right), m \neq n \\ -\frac{k\eta_0\Delta\rho}{4}\left[1 + i\frac{2}{\pi}\log\left(\frac{\gamma k\Delta\rho}{4e}\right)\right], m = n \end{cases} \quad \text{(SBC)} \qquad (7a)$$

$$Z_{nm} \cong \begin{cases} -\frac{ik\Delta\rho}{4} H_1^{(1)}\left(k|\boldsymbol{\rho}_\mathbf{n} - \boldsymbol{\rho}_\mathbf{m}|\right)(\hat{\mathbf{n}}_\mathbf{m} \cdot \hat{\boldsymbol{\rho}}_\mathbf{mn}), m \neq n \\ 0.5, m = n \end{cases} \quad \text{(HBC)} \qquad (7b)$$

where $\Delta\rho$ is the segment length, $\eta_0 \approx 120\pi$ is the intrinsic impedance of free space, $H_0^{(1)}$ and $H_1^{(1)}$ are the first kind Hankel function with order zero and one, respectively, $\gamma \approx 1.781$ is the exponential of the Euler constant, $\hat{\mathbf{n}}_\mathbf{m}$ denotes the unit normal vector of the segment at $\boldsymbol{\rho}_\mathbf{m}$, and $\hat{\boldsymbol{\rho}}_\mathbf{mn}$ is the unit vector in the direction from source $\boldsymbol{\rho}_\mathbf{m}$ to the receiving element $\boldsymbol{\rho}_\mathbf{n}$. While considering the effects of segment currents between top and bottom wedge, the scattered fields are

$$E_z^{sc}(\boldsymbol{\rho}_\mathbf{n}) \cong -\frac{k\eta_0\Delta\rho}{4}\sum_{m=1}^{2N} I_m H_0^{(1)}\left(k|\boldsymbol{\rho}_\mathbf{n} - \boldsymbol{\rho}_\mathbf{m}|\right) \text{ (SBC)} \qquad (8a)$$

$$H_z^{sc}(\boldsymbol{\rho}_\mathbf{n}) \cong -\frac{ik\Delta\rho}{4}\sum_{m=1}^{2N} I_m H_1^{(1)}\left(k|\boldsymbol{\rho}_\mathbf{n} - \boldsymbol{\rho}_\mathbf{m}|\right)(\hat{\mathbf{n}}_\mathbf{m} \cdot \hat{\boldsymbol{\rho}}_\mathbf{mn}) \text{ (HBC)} \qquad (8b)$$

Finally, the incident field at the observer is added and total fields are obtained.

IV. Finite Difference Time Domain Modeling

The multi-step FDTD-based diffraction modeling introduced in [12] under the line source illumination is general and yields diffracted fields under any *source/observer locations*. The FDTD-based Matlab package *WedgeFDTD* can be used in the visualization of diffracted fields using this multi-step FDTD procedure [13]. The FDTD procedure for SSI is as follows [12-13]:

- First, the wedge scenario is modeled with FDTD and total fields (i.e., incident, reflected, and diffracted field components for $0 \le \varphi < \pi - \varphi_0$; incident and diffracted field components for $\pi - \varphi_0 \le \varphi < \pi + \varphi_0$; and only the diffracted fields for $\pi + \varphi_0 \le \varphi < \alpha$, see, Table 1).
- Then, FDTD is run for the infinite-plane scenario ($\alpha = 180°$) which yields total fields on the upper half plane ($0 \le \varphi < \pi$). Since there is no edge or tip, the total fields include only incident and reflected fields; and do not contain diffracted fields.
- Finally, the free-space scenario is run with FDTD and only incident fields are recorded.
- The FDTD simulation is run separately for each of these three scenarios and time-domain data are recorded. Subtracting the time data of the second scenario from the first scenario for ($0 \le \varphi < \pi - \varphi_0$); and the time data of the third scenario from the first scenario for ($\pi - \varphi_0 \le \varphi < \pi + \varphi_0$) will yield diffracted-only fields all around the wedge.

Note that, the three step procedure is enough to obtain diffracted fields under SSI condition, but another infinite plane consisting of two half-planes oriented along the angles $\varphi = \alpha - \pi$ and $\varphi = \alpha$ is required for DSI.

V. Examples and Comparisons

Examples using this novel MoM procedure are shown in Figs. 2 and 3, where MoM-extracted diffracted fields for both polarizations (SBC and HBC) are compared against the analytical reference solution as well as the UTD model and the FDTD method.

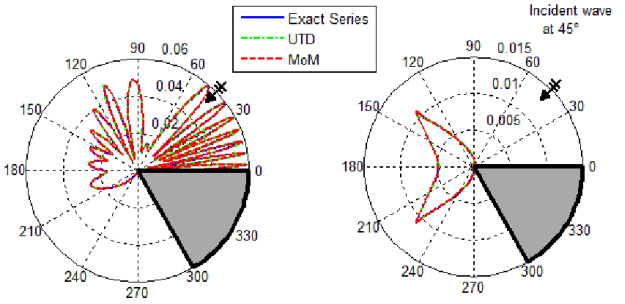

Fig. 2. (Left) Total fields and (Right) diffracted fields around PEC wedge as a function of angles at 30 MHz using exact series, UTD, MoM, and FDTD solutions: $\alpha = 300°$, $r = 50$ m, $r_0 = 100$ m, $\varphi_0 = 45°$, (TM/SBC case).

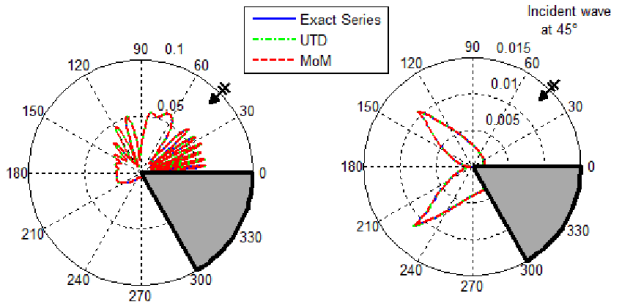

Fig. 3. (Left) Total fields and (Right) diffracted fields around PEC wedge as a function of angles at 30 MHz using exact series, UTD, MoM, and FDTD solutions: $\alpha = 300°$, $r = 50$ m, $r_0 = 100$ m, $\varphi_0 = 45°$, (TE/HBC case).

A non-penetrable wedge with 60° interior angle is taken into account in Fig. 2. Soft BC (TM_z case) is assumed. Total and diffracted fields vs. angle around the tip of the wedge on a circle with 5λ-radius are plotted. The wedge is illuminated by a line source located 10λ-distance with $\varphi_0 = 45°$. Infinite wedge faces are truncated in 100λ and segment lengths are chosen λ/20. MoM results are compared with exact series representation, UTD model, and FDTD model. Total field vs. angle plots on the left show the three regions clearly. As observed, very good agreement is obtained with MoM modeling even with these rough discretization parameters.

The second example in Fig. 3 belongs to a non-penetrable wedge with the same interior angle and illumination angle as above, but HBC is used. As observed, the agreement among the models is also very good.

VI. CONCLUSIONS

A novel Method of Moment (MoM) modeling is introduced for the calculation of diffracted fields in the frequency domain. Electromagnetic wave scattering from a non-penetrable wedge is taken into account and the edge-diffracted fields are extracted numerically and compared with the FDTD method. The results are also validated against analytical reference solutions as well as the Uniform Theory of Diffraction (UTD). Like FDTD, this two-step MoM approach can be used to obtain the diffraction coefficients of scatterers with arbitrary shape and decomposition (e.g., loss-free and lossy dielectrics, metamaterials, etc.). Higher order diffraction effects can also be modeled, and, for example, double diffraction coefficients of multiple tips can be obtained.

REFERENCES

[1] C.A. Balanis, Advanced Engineering Electromagnetics, John Wiley & Sons, Inc., USA, 2012.

[2] P. Ya. Ufimtsev, Fundamentals of the Physical Theory of Diffraction, Wiley & Sons, Inc., USA, 2007.

[3] F. Hacivelioglu, L. Sevgi, and P. Ya. Ufimtsev, "Wedge diffracted waves excited by a line source: exact and asymptotic forms of fringe waves," IEEE Trans. on Antennas and Propagat., vol. 61 (9), pp. 4705-4712, Sep. 2013.

[4] C. Balanis, L. Sevgi, and P. Ya Ufimtsev, "Fifty years of high frequency asymptotics," RFMiCAE, International Journal on RF and Microwave Computer-Aided Engineering, vol. 23 (4), pp. 394-402, July 2013.

[5] G. Pelosi, Y. Rahmat-Samii, and J. Volakis, "High frequency techniques in diffraction theory: 50 years of achievements in GTD, PTD, and related approaches", IEEE Antennas Propag. Mag., vol. 55 (3), pp. 16-17, June 2013.

[6] P. Ya. Ufimtsev, "The 50-year anniversary of PTD: comments on the PTD's origin and development," IEEE Antennas Propag. Mag., vol. 55 (3), pp.18-28, June 2013.

[7] Y. Rahmat-Samii, "GTD, UTD, UAT, and STD: a historical revisit and personal observations," IEEE Antennas Propag. Mag., vol. 55 (3), pp. 29-40, June 2013.

[8] G. Pelosi and S. Selleri, "The wedge-type problem: the building brick in high-frequency scattering from complex objects," IEEE Antennas Propag. Mag., vol. 55 (3), pp. 41-60, June 2013.

[9] F. Hacivelioglu, M. A. Uslu, and L. Sevgi, "A Matlab-based virtual tool for the electromagnetic wave scattering from a perfectly reflecting wedge", IEEE Antennas Propag. Mag., vol. 53 (6), pp. 234-243, Dec. 2011.

[10] K. Yee, "Numerical solution of initial boundary value problems involving Maxwell's equations in isotropic media," IEEE Trans. on Antennas and Propagat., vol. 14 (3), pp. 302–307, May 1966.

[11] G. Stratis, V. Anantha, A. Taflove, "Numerical calculation of diffraction coefficients of generic conducting and dielectric wedges using FDTD," IEEE Trans. on Antennas and Propagat., vol. 45 (10), pp. 1525–1529, Oct. 1997.

[12] G. Cakir, L. Sevgi, and P. Ya. Ufimtsev, "FDTD modeling of electromagnetic wave scattering from a wedge with perfectly reflecting boundaries: comparisons against analytical models and calibration," IEEE Trans. on Antennas and Propagat., vol. 60 (7), pp. 3336-3342, July 2012.

[13] M. A. Uslu and L. Sevgi,"Matlab-based virtual wedge scattering tool for the comparison of high frequency asymptotics and FDTD method," Applied Computational Electromagnetics Society Journal, vol. 27 (9), pp. 697-705, 2012.

[14] R. F. Harrington, Field Computation by Moment Method, New York: IEEE Press, (First Ed. 1968), 1993.

[15] E. Arvas and L. Sevgi, "A tutorial on the method of moments," IEEE Antennas Propag. Mag., vol. 54 (3), pp. 260–275, June 2012.

[16] G. Apaydin and L. Sevgi, "A canonical test problem for computational electromagnetics (CEM): Propagation in a parallel-plate waveguide," IEEE Antennas Propag. Mag., vol. 54 (4), pp. 290-315, Aug. 2012.

[17] G. Apaydin and L. Sevgi, "Method of moments (MoM) modeling for resonating structures: propagation inside a parallel plate waveguide," Applied Computational Electromagnetics Society Journal, vol. 27 (10), pp. 842-849, Oct. 2012.